J. Fluid Mech. (1972), *vol.* 54, *part* 3, *pp.* 565–575
Printed in Great Britain

Experiments on the flow past spheres at very high Reynolds numbers

By ELMAR ACHENBACH
Kernforschungsanlage Jülich GmbH, Jülich, Germany

(Received 16 October 1971 and in revised form 5 March 1972)

The present work is concerned with the flow past spheres in the Reynolds number range $5 \times 10^4 \leqslant Re \leqslant 6 \times 10^6$. Results are reported for the case of a smooth surface. The total drag, the local static pressure and the local skin friction distribution were measured at a turbulence level of about 0·45 %. The present results are compared with other available data as far as possible. Information is obtained from the local flow parameters on the positions of boundary-layer transition from laminar to turbulent flow and of boundary-layer separation. Finally the dependence of friction forces on Reynolds number is pointed out.

1. Introduction

In the Nuclear Research Laboratories at Jülich a gas-cooled high-temperature reactor working with spherical fuel elements is being developed. The spheres, which have a diameter of 0·06 m, are transported pneumatically through tubes (diameter $d_t = 0{\cdot}065$ m) under the conditions of the primary cooling gas, i.e. helium at 40 bars and 250 °C. Because of the high pressure of the system large Reynolds numbers are to be expected. It was supposed that, during the transporting process, flow around the sphere could reach the critical state, which is characterized by a low drag coefficient and unsteady flow conditions. In the preliminary tests reported herein the influence of high blockage ratios on the drag of spheres was not considered; only the flow around smooth spheres in a free stream at high Reynolds numbers was studied.

Though numerous investigations on this topic have been made there is a lack of experimental data at high Reynolds numbers. For instance only Bacon & Reid (1924) have measured the drag coefficient of spheres beyond $Re = 10^6$. Information on local skin friction is also incomplete: Fage's (1936) measurements up to $Re = 4{\cdot}25 \times 10^5$ ranged only from the point where the circumferential angle $\phi = 50°$ to the vicinity of the separation point, whereas Wadsworth's (1958) investigations yielded only qualitative results, as he did not calibrate his probe. Moreover, the available data differ from one another because of the many parameters which influence the flow. These main parameters are: the turbulence level of the flow, the effect of the supports, surface roughness, tunnel blockage and Mach number. Around the critical flow regime, in which the boundary layer is extremely sensitive, these influences have a large effect, so the experimental results of different authors show significant deviations from one another.

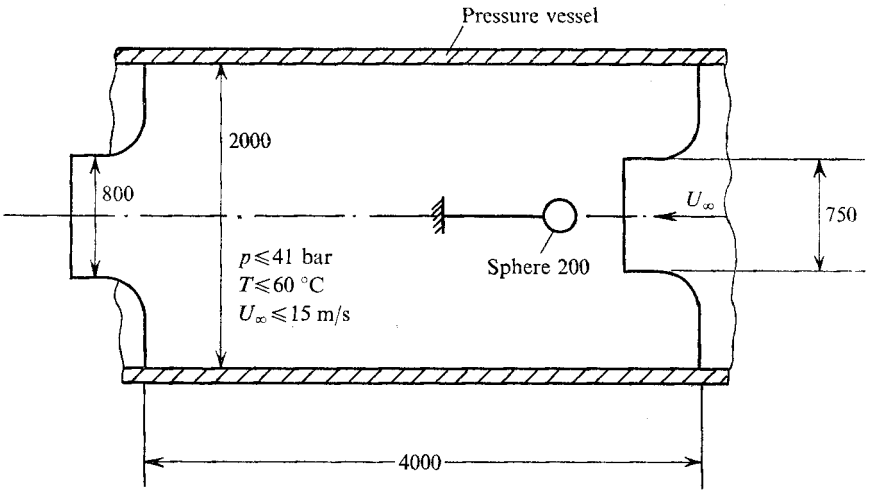

FIGURE 1. Sketch of the test section of the high-pressure wind tunnel, dimensions in mm.

In our investigations we have tried to define the conditions and to keep the parameters constant as far as possible in order to focus attention on the effect of Reynolds number. Thus we measured the total drag and the local static pressure and skin friction distribution.

2. Experimental apparatus and measurement techniques

The high Reynolds numbers were achieved in a high-pressure wind tunnel, in which pressures up to 40 bars could be obtained. The maximum undisturbed velocity of the air jet to which the spheres were exposed was $U_\infty \approx 15$ m/s. The turbulence level of the jet was measured with a hot wire; a value of about 0·45 % was obtained and was independent of U_∞. Figure 1 shows a sketch of the test arrangement. The experiments at lower Reynolds numbers were carried out in an atmospheric test rig of the same geometrical size as the high-pressure wind tunnel. The maximum velocity was $U_\infty = 33$ m/s. To avoid wall interference the spheres, supported from the rear, were installed at the exit of the nozzle in the free air jet. The diameter of the sting was $0{\cdot}1d$, where d is the diameter of the sphere. The total drag D was determined by means of a hollow 200 mm test sphere made out of aluminium, the surface being polished. Figure 2 shows how the test body was supported and where the strain gauges were mounted to measure the drag forces. This balance operating through a strain gauge bridge could easily be calibrated by loading it with weights. The calibration curve was exactly linear. Zero-point drift was almost eliminated by keeping the gas temperature constant to within $\pm 0{\cdot}5$ °C.

Another constructional arrangement, a sketch of which is shown in figure 3, was chosen to measure the local static pressure and the skin friction distribution. The hollow brass sphere ($d = 175$ mm) consisted of two outer fixed parts and a central ring, which could be rotated around an axis transverse to the flow, i.e. along a meridian, by an electric motor mounted on the inside. The annular

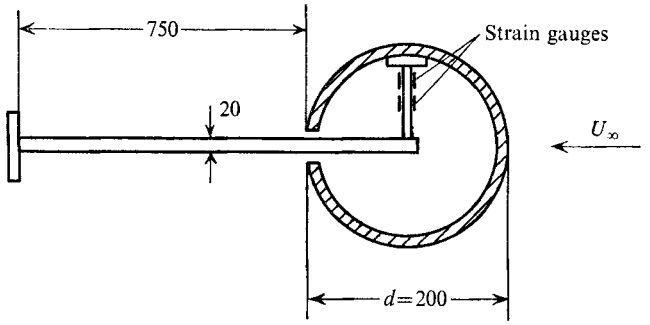

FIGURE 2. Experimental arrangement for the measurement of the total drag forces, dimensions in mm.

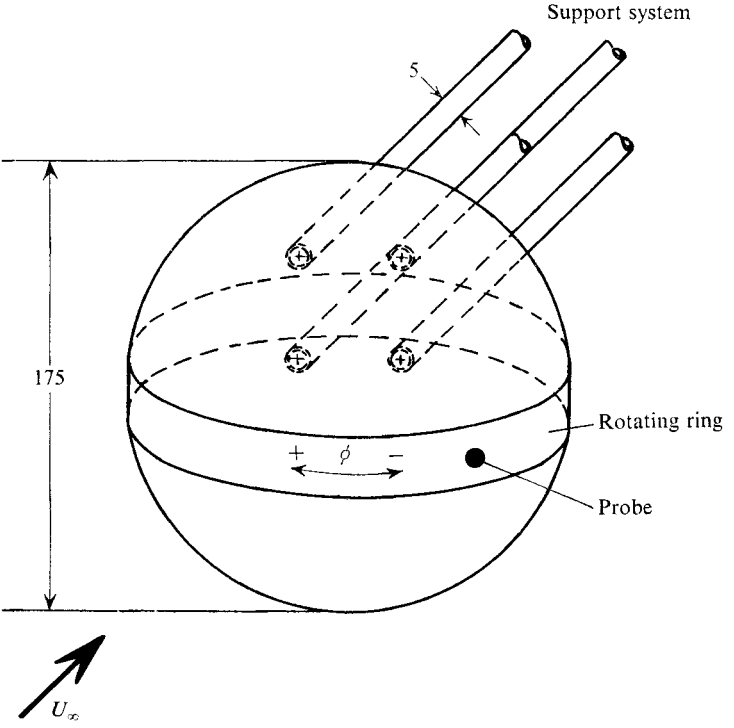

FIGURE 3. Test sphere for the determination of the local flow parameters, dimensions in mm.

segment supported the probes, which thus could be positioned at any point of the meridian. The position was indicated by means of a precision potentiometer. The sphere itself was held by four tubes, 5 mm in diameter, arranged in a 35 mm square. Two of these tubes supported each of the outer shells, which were connected to one another by a shaft.

The skin friction probe was of the same type as that described in a previous paper (Achenbach 1968). The principle of operation is based on the fact that the pressure difference across a small obstacle exposed to the boundary layer depends only on the wall shear stresses τ_0. The present probe consists of a small edge which projects only some hundredths of a millimetre into the boundary layer. The

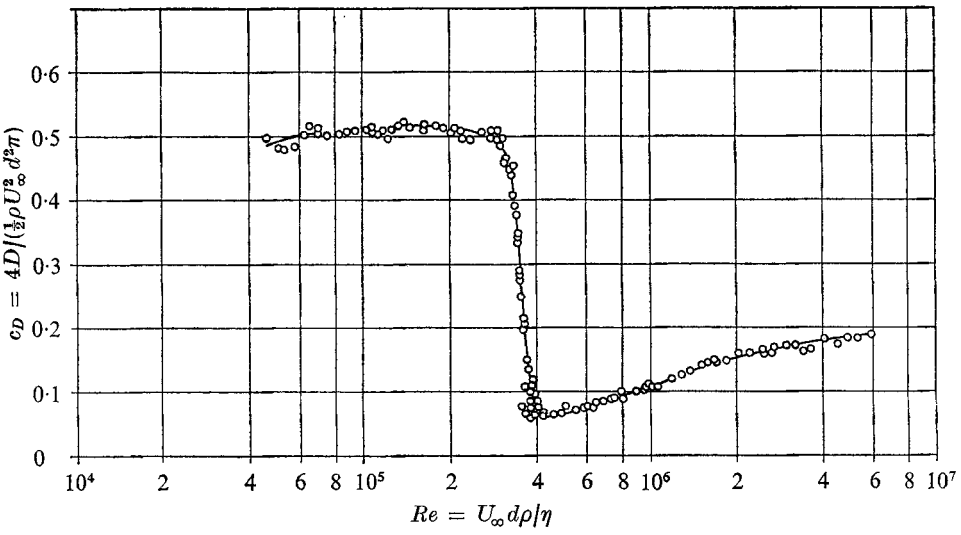

FIGURE 4. Drag coefficient of the smooth sphere as a function of Reynolds number.

pressure difference Δp_e across the edge, which is mounted perpendicular to the flow, is measured by means of two extremely narrow slots in front of and behind the obstacle. The method of calibrating the probe was analogous to that used for the circular cylinder in a cross flow. The three-dimensional boundary-layer calculation which was necessary to determine the wall shear stresses and hence the calibration curve was carried out according to the method reported by Schlichting (1964). Unfortunately this method yields a calibration curve only for the case of laminar boundary layers. In the absence of a better estimate the 'laminar curve' was used also for the turbulent part of the boundary layer. The error thus introduced could not be estimated, therefore the results referring to the turbulent flow are of a qualitative character.

3. Results

Figure 4 represents the drag coefficient $c_D = 4D/[\frac{1}{2}\rho U_\infty^2 \pi d^2]$ of the smooth sphere as a function of the Reynolds number $Re = U_\infty d\rho/\eta$. The characteristic quantities are the diameter d of the sphere and the free-stream velocity U_∞. ρ and η are respectively fluid density and dynamic viscosity. The results were obtained by a direct measurement of the drag force by means of strain gauges. As the test arrangement was sensitive to asymmetries in the flow the results were checked by rotating the support system by 90° around the axis parallel to the flow. The experiments have been conducted at variable system pressure. If the steps $p = 41, 21, 11, 5, 2{\cdot}5$ and 1 bar are chosen the experimental values obtained at neighbouring pressure levels overlap. From the curve of c_D versus Re four ranges can be distinguished (see also the sketch in figure 5). In the subcritical flow the drag coefficient is nearly independent of Reynolds number. The next range, which is called the critical one, is characterized by a rapid drop of the drag coefficient, the minimum being reached at the critical Reynolds number

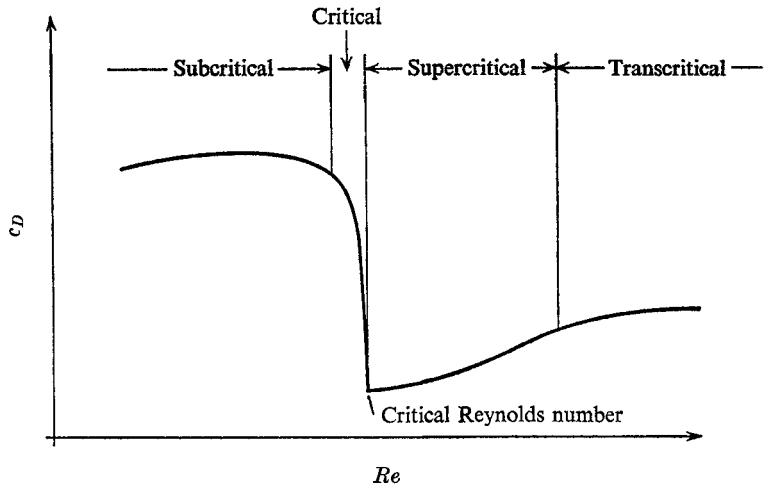

FIGURE 5. On the explanation of the four flow regimes.

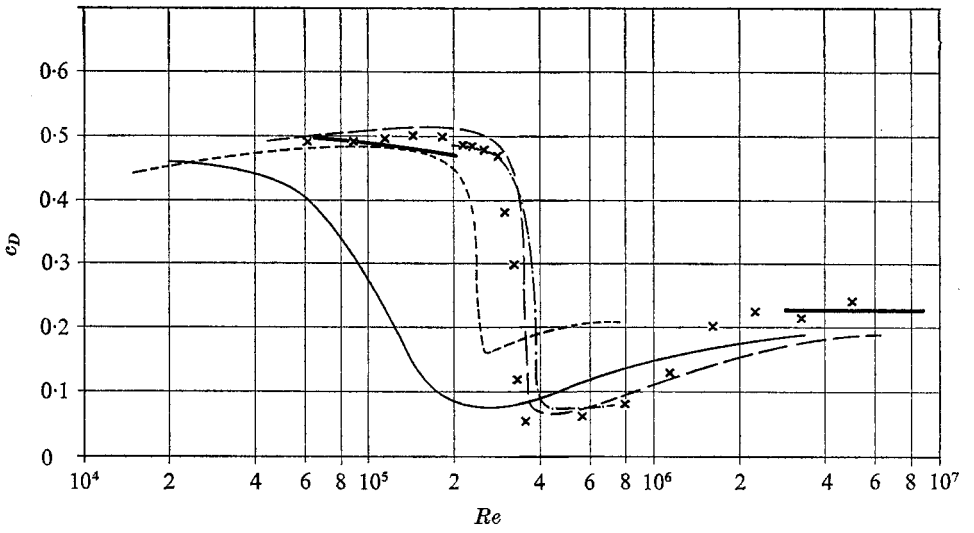

FIGURE 6. Drag coefficient of the sphere as a function of Reynolds number; comparison with literature. – – –, Wieselsberger (1922); ——, Bacon & Reid (1924); —·—, Millikan & Klein, free-flight (1933); ——, Maxworthy (1969). Present results: ——, from strain gauges; ×, from integration.

$Re \approx 3{\cdot}7 \times 10^5$. With further increase of the Reynolds number, c_D slowly increases again (supercritical flow) and it seems that the curve is going to reach another maximum. The transition from supercritical to transcritical flow is rather floating. To define the boundary it is advantageous to make use of the local skin friction distribution. As will be described later, the transcritical flow regime is indicated by the shifting of the transition point from $\phi_t = 95°$ in direction of the stagnation point when the Reynolds number is increased.

Figure 6 gives a comparison of the present results with those of Wieselsberger (1922), Bacon & Reid (1924), Millikan & Klein (1933) and Maxworthy (1969).

The flow in Wieselsberger's experiments seems to be influenced by the support system, as c_D diminishes only down to a critical value of 0·15. Results referring to a very low turbulence level are reported by Millikan & Klein, whose free-flight tests are cited herein. Their results agree very well with ours except in the critical flow range. On account of the low turbulence level their critical Reynolds number is about 10 % higher than ours. Bacon & Reid used a pressurized wind tunnel for their experiments, as we did. Thus they obtained Reynolds numbers up to $3{\cdot}6 \times 10^6$ with a test sphere with $d = 0{\cdot}200$ m. From the shape of the curve, i.e. low critical Reynolds number and gradual decrease of the drag coefficient in the critical flow regime, it must be concluded that the turbulence level was quite high. At very large Reynolds numbers this influence of the turbulence level seems to diminish. Perhaps the turbulence level of the incident flow was comparable with that of the turbulent boundary layer on the sphere.

Finally, recent work of Maxworthy (1969) should be mentioned. From experiments with Re up to 2×10^5, he tried to get information on the drag coefficient at transcritical flow conditions by mounting a boundary-layer trip at $\phi = 55°$. The value for $Re \approx 10^7$ is predicted by this method to be about 15 % higher than the value obtained by an extrapolation of the present experimental results. On consideration of figure 8 (below) it is obvious that the natural transition from laminar to turbulent flow occurs at $\phi_s = 55°$ for $Re = 6 \times 10^6$. The corresponding drag coefficient is $c_D = 0{\cdot}19$. However, Maxworthy's experiments, carried out with a boundary-layer trip at $\phi = 55°$, yielded a transcritical drag coefficient of $c_D = 0{\cdot}23$. This evidence seems to indicate that the energy distribution in the boundary layer is different in both cases, though transition occurs at the same position.

The crosses in figure 6 represent results obtained by integration of the local static pressure and skin friction. The agreement with the direct measurement of the drag force is good in some regions. In the critical and transcritical flow range significant deviations become evident. Probably the slots which are incorporated in the rotating segment act as a boundary-layer trip.

Figure 7 gives information on the flow conditions in the boundary layer as a function of Reynolds number. As well as the experimental results the theoretical curves are included for comparison. The theoretical pressure distribution comes from the potential theory of the flow around spheres. Based on this pressure distribution the local skin friction can be calculated according to the series-method described by Schlichting (1964).

From our numerous experimental results only one example was selected for each flow range defined above. In the subcritical flow regime represented by the curves $Re = 1{\cdot}62 \times 10^5$ the boundary layer separates laminarly at $\phi_s = 82°$. For angles greater than ϕ_s the skin friction is negative, which means a recirculation of the flow. The corresponding static pressure distribution already deviates considerably from the theoretical curve at $\phi \approx 30°$. The base pressure is the lowest compared with those for the other results shown in figure 7.

For $Re > 2 \times 10^5$ the point of laminar boundary-layer separation shifts downstream. At $Re = 2{\cdot}8 \times 10^5$ the value of $\phi_s \approx 95°$ is reached. With further increase of Reynolds number the boundary layer no longer separates at $\phi = 95°$, but has

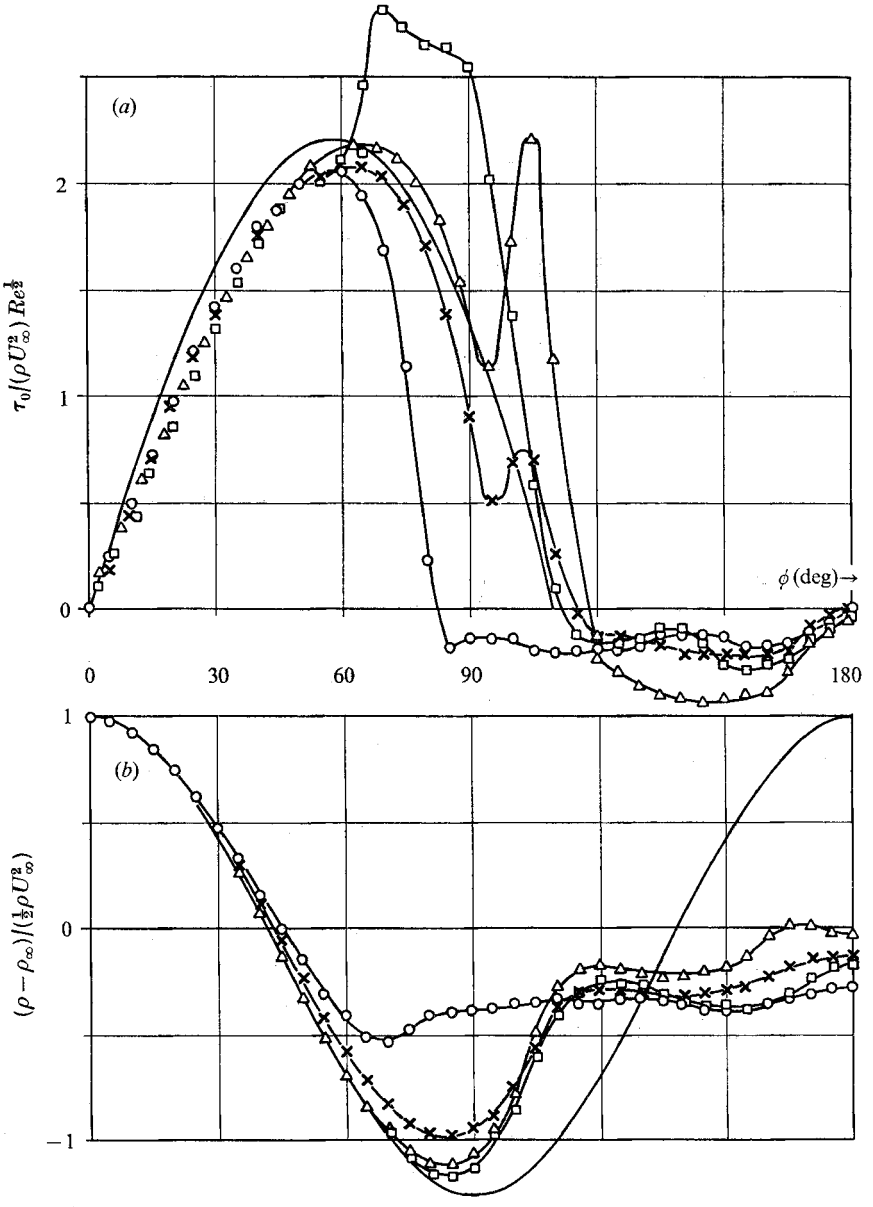

FIGURE 7. (*a*) Local skin friction and (*b*) static pressure distribution for the smooth sphere at variable Reynolds numbers. ——, theory. Experiment: —○—, $Re = 1{\cdot}62 \times 10^5$; —×—, $Re = 3{\cdot}18 \times 10^5$; —△—, $Re = 1{\cdot}14 \times 10^6$; —□—, $Re = 5{\cdot}00 \times 10^6$.

at this position a minimum in the skin friction, which is followed by a new increase in the wall shear stress. As the value of the wall shear stress at minimum skin friction is low, it was assumed, without looking for other evidence, that laminar intermediate separation occurs and is followed by a transition in the free shear layer from a laminar to a turbulent flow. Further downstream the turbulent shear layer reattaches to the wall. This phenomenon of forming a separation bubble was regarded as typical for the critical flow regime. The step width of $\Delta\phi = 5°$,

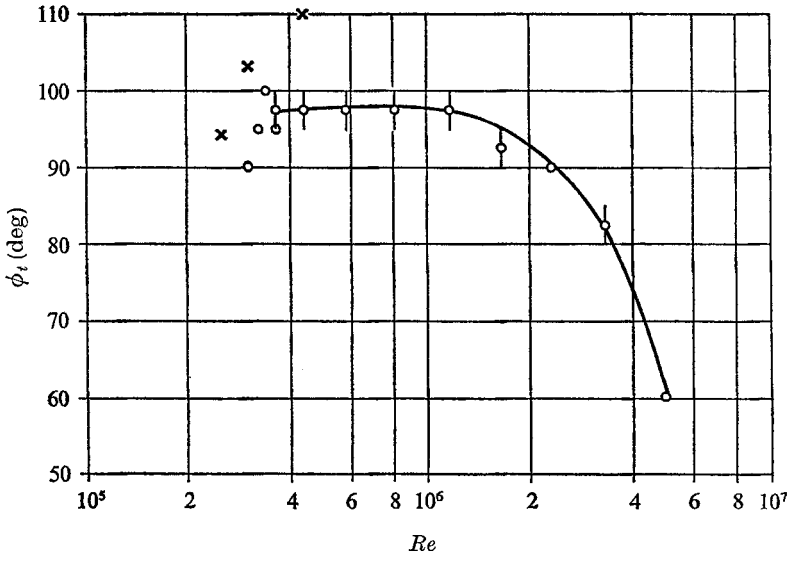

FIGURE 8. Position of boundary-layer transition from laminar to turbulent flow for smooth spheres. ×, Fage (1936); ○, present results.

which was chosen to pick up the local quantities, was too large to describe the shape of the pressure and skin friction curves in more detail. Therefore we did not detect the almost constant pressure region at the position of the separation bubble shown, for instance, by Fage (1936). Perhaps this is also the reason why we did not detect the point of zero skin friction at the position of the laminar intermediate separation. However, it did not seem to be reasonable to diminish the step width, as significant fluctuations of the static pressure and skin friction, which lead to difficulties of the averaging readout process, were observed in the region between $\phi \approx 90°$ and the downstream point of maximum skin friction (see figure 7, $Re = 3{\cdot}18 \times 10^5$). The unsteady behaviour of the flow could be recognized as pressure transducers of small, constant volume (Texas Instruments) were used, the damping of which is considerably less than that of other manometers operating, for instance, on the displacement of a fluid.

On exceeding the critical Reynolds number, which may be defined as that at which c_D is minimum, the supercritical range follows. In this range, which extends to about $Re = 1{\cdot}5 \times 10^6$, the transition is observed to be locally fixed downstream of the main cross-section. As is shown in the curve referring to $Re = 1{\cdot}14 \times 10^6$ the wall shear stress at $\phi = 95°$ is obviously positive. From this it is concluded that the transition from laminar to turbulent flow occurs immediately without formation of a separation bubble. When the Reynolds number is increased beyond $Re = 1{\cdot}5 \times 10^6$ the transition point shifts upstream. Now the transcritical flow state is reached, and is characterized by an immediate transition from a laminar to a turbulent boundary layer in the front part of the sphere.

The evaluation of the skin friction measurements is continued in figures 8 and 9, which show respectively the position of transition and of boundary-layer separation. With regard to the transition from laminar to turbulent flow there are practically no data available except a few points reported by Fage (1936)

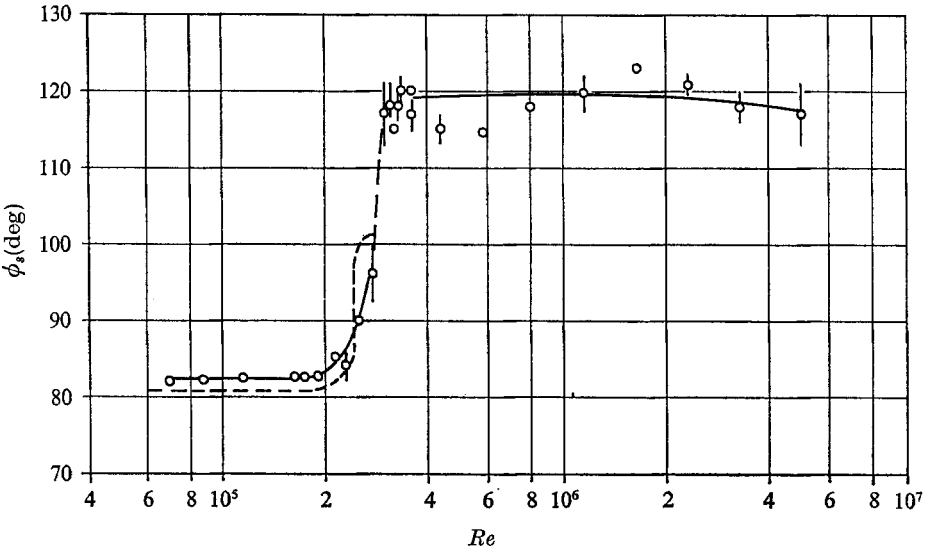

FIGURE 9. Position of boundary-layer separation for smooth spheres. ———, Raithby & Eckert (1968); ○, present results.

(crosses in figure 8). His values, which come from the static pressure distribution (at the position of transition no data of skin friction are reported) show satisfactory agreement with our results. From the present experimental curve it can be seen that up to $Re \approx 1{\cdot}5 \times 10^6$ the transition occurs downstream of the main cross-section. This was assumed to be characteristic for the critical and supercritical flow regime. For Reynolds numbers greater than $Re = 1{\cdot}5 \times 10^6$ (transcritical range) the transition point moves towards the front stagnation point. The circles represent the mean value of the angles of transition ϕ_t measured at two opposite positions on a meridian. The vertical lines indicate the deviation of the experimental results from the mean value.

In the literature the information on boundary-layer separation is more complete than that on boundary-layer transition. The field of interest in most cases is the critical flow range and particularly the influence of turbulence level on the critical Reynolds number. The methods preferred are flow visualization and the application of Preston or Stanton tubes. In figure 9, which shows the position of boundary-layer separation as a function of Reynolds number, the results of Raithby & Eckert (1968) referring to the rear support and with a turbulence level of 0·65 % are also plotted. In the subcritical flow regime the agreement with our results is satisfactory. As is demonstrated by the work of Raithby & Eckert, the results of Wadsworth (1958) are not comparable with ours because he used cross-flow support, which leads to unsymmetrical flow. Maxworthy (1969) found in his investigations that the boundary layer separates at $\phi_s = 82{\cdot}5°$ in the subcritical flow range. This is in good agreement with our results.

Figure 10 is also derived from the experimental determination of local static pressure and skin friction. Integration of the local parameters yields the percentage contribution of friction forces to the total drag on the sphere. In the subcritical flow regime this percentage decreases as $Re^{-0{\cdot}5}$ whilst c_D is nearly

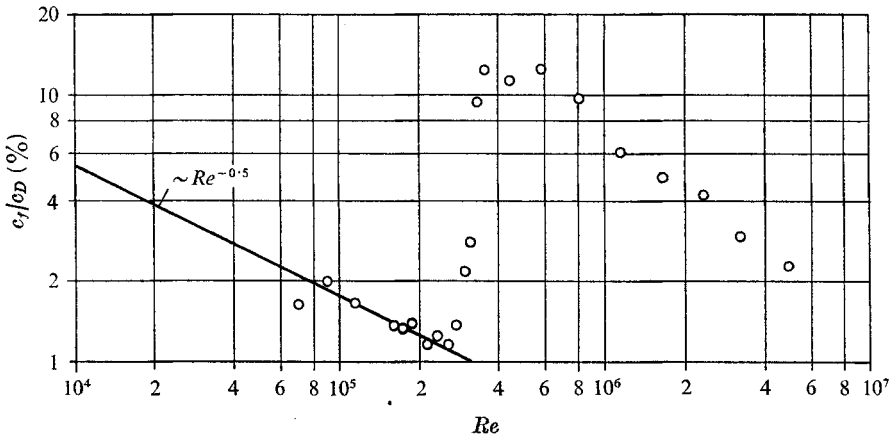

FIGURE 10. Friction forces as a percentage of the total drag for smooth spheres.

constant. In the critical flow range the contribution of friction increases strongly up to the considerable value of 12·5 % as a result of the abrupt drop in the drag coefficient. Subsequently the friction rate is observed to decrease again. The slope of the curve is now smaller than $-0{\cdot}5$, since c_D is growing with increasing Reynolds number.

4. Critical remarks

The experimental results reported here have been carefully checked for possible influences other than changes in the Reynolds number. The turbulence level of the incident flow was constant for all test runs. Therefore the observed variations of flow behaviour cannot be influenced by this parameter. The test spheres were supported from the rear by a sting of small diameter because this was expected to give least effect on the flow. For the same reason, a filigree support was constructed to fasten the more complicated sphere which was used for the determination of the local flow parameters. To achieve high Reynolds numbers large sphere diameters must be used. This, however, gives rise to the problem of tunnel blockage. We tried to overcome this difficulty by putting the spheres in the free air jet. The effect of Mach number described by Naumann (1953) could completely be excluded as the value $M = 0{\cdot}1$ was never exceeded. At, for instance, the maximum Reynolds number, which was obtained in the high-pressure wind tunnel, the Mach number was even lower than $M = 0{\cdot}05$.

The surface of the spheres should be highly polished to avoid effects of surface roughness. This condition could easily be fulfilled for the total drag measurements. However, the sphere used for the local tests contained two circumferential slots formed by the rotating ring element. These are noticeable obstacles for the flow, as is demonstrated by the shape of the c_D versus Re curve given by integration in figure 6. The effect is particularly obvious in the critical and transcritical flow regimes. Nevertheless, the local skin friction and static pressure distributions presented in figure 7 reveal instructively how the development of the boundary layer depends on Reynolds number. The problems arising from the techniques

used in measuring the local skin friction have already been considered in the previous paper (Achenbach 1968). The danger of premature boundary-layer separation caused by the skin friction probe is generally real. In the present case, however, this effect remains concealed because of the disturbances which are generated by the slots formed by the rotating segment.

This investigation was performed at the Institut für Reaktorbauelemente, Kernforschungsanlage Jülich, Germany. The author wishes to thank Dr C. B. von der Decken, Director of the Institute, for his great interest in this work and for the opportunity to carry out the tests. He also wants to acknowledge the active support of all his co-workers. Gratitude is expressed particularly to H. Gillessen, F. Hoffmanns, H. Reger and W. Schmidt for their valuable assistance.

REFERENCES

Achenbach, E. 1968 Distribution of local pressure and skin friction around a circular cylinder in cross-flow up to $Re = 5 \times 10^6$. *J. Fluid Mech.* **34**, 625–639.

Bacon, D. L. & Reid, E. G. 1924 The resistance of spheres in wind tunnels and in air. *Nat. Adv. Com. Aero. Rep.* no. 185.

Fage, A. 1936 Experiments on a sphere at critical Reynolds numbers. *Aero. Res. Counc. R. & M.* no. 1766.

Maxworthy, T. 1969 Experiments on the flow around a sphere at high Reynolds numbers. *J. Appl. Mech., Trans. A.S.M.E.* E **36**, 598–607.

Millikan, C. B. & Klein, A. L. 1933 The effect of turbulence. An investigation of maximum lift coefficient and turbulence in wind tunnels and in flight. *Aircraft Eng.* **5**, 169–174.

Naumann, A. 1953 Luftwiderstand der Kugel bei hohen Unterschallgeschwindigkeiten. *Allgemeine Wärmetechnik*, **4**, 217–221.

Raithby, G. D. & Eckert, E. R. G. 1968 The effect of support position and turbulence intensity on the flow near the surface of a sphere. *Wärme- und Stoffübertragung*, **1**, 87–94.

Schlichting, H. 1964 *Grenzschicht-Theorie*, pp. 215–220. Karlsruhe: Braun.

Wadsworth, J. 1958 The experimental examination of the local heat transfer on the surface of a sphere when subjected to forced convective cooling. *Nat. Res. Counc. Can. Rep.* MT-39.

Wieselsberger, C. 1922 Weitere Feststellungen über die Gesetze des Flüssigkeits- und Luftwiderstandes. *Phys. Z.* **23**, 219–224.